

PAPER • OPEN ACCESS

## Evaporation of confined droplet between parallel chips with varying gap at room temperature

To cite this article: Vikas Dubey 2022 *J. Micromech. Microeng.* **32** 075001

View the [article online](#) for updates and enhancements.

### You may also like

- [Biocompatible bonding of a rigid off-stoichiometry thiol-ene-epoxy polymer microfluidic cartridge to a biofunctionalized silicon biosensor](#)  
Linda Sønstevold, Mukesh Yadav, Nina Bjørk Arnfinnsdottir et al.
- [Vibration analysis of MEMS vibrating mesh atomizer](#)  
Pallavi Sharma and Nathan Jackson
- [Micromachined threshold inertial switches: a review](#)  
Qiu Xu and Mohammad I Younis

The advertisement is divided into two main sections. The left section is for the "249th ECS Meeting" held from May 24-28, 2026, in Seattle, WA, US, at the Washington State Convention Center. It features a logo for "SUSTAINABLE TECHNOLOGIES" with a stylized globe and leaves. The right section is for "Spotlight Your Science" with a submission deadline of December 5, 2025. It includes a large "SUBMIT YOUR ABSTRACT" button.

**ECS** The Electrochemical Society  
Advancing solid state & electrochemical science & technology

**SUSTAINABLE TECHNOLOGIES**

**249th ECS Meeting**  
May 24-28, 2026  
Seattle, WA, US  
Washington State Convention Center

**Spotlight Your Science**

**Submission deadline:**  
**December 5, 2025**

**SUBMIT YOUR ABSTRACT**

# Evaporation of confined droplet between parallel chips with varying gap at room temperature

Vikas Dubey 

System Packaging, Fraunhofer Institute for Electronic Nanosystems (ENAS), Technologie-Campus 3, Chemnitz, 09126, Germany

E-mail: [vikasace10@gmail.com](mailto:vikasace10@gmail.com)

Received 24 January 2022, revised 16 April 2022

Accepted for publication 11 May 2022

Published 30 May 2022



## Abstract

A theoretical study and experimental validation of the evaporation of a droplet confined between two parallel square chips with a free-standing top chip over a water meniscus is presented in this article. The analytical model describes the surface area of a negatively curved liquid–air interface, and the evaporation model was thus solved for this case. The dynamics of decreasing the gap between the two parallel chips show a linear dependency in time at room temperature. Two main regimes are observed in this case, the constant wetted area regime and the varying wetted area regime. The theoretical study was lastly validated through experiments.

Supplementary material for this article is available [online](#)

**Keywords:** evaporation, assembly, parallel plates, droplet, 3D integration, self-assembly, microassembly

(Some figures may appear in colour only in the online journal)

## 1. Introduction

Evaporation studies of sessile drop on surfaces and suspended droplets have been conducted by several researchers [1–14]. Such study is key towards building an understanding of various complex phenomena such as coffee rings [1], clouds, fog [3], etc. The main cause of evaporation of droplets is mainly attributed to concentration gradient [4, 9]. Depending on the affinity of the surface for a sessile droplet, there are three evaporation modes, namely: constant contact radius [10, 11], constant contact angle [12–14], and a mixed-mode.

The liquid confined between two surfaces plays a major role in the bonding of surfaces such as wafer-to-wafer bonding [15], designing of the saucer, capillary gripper [16], and

various other surface designs [17]. In the case of bonding between the surfaces, the droplet present between the surfaces will eventually evaporate with time. Clement and Leng studied the evaporation of a liquid droplet between two parallel plates at a constant gap of  $50\ \mu\text{m}$  [18, 19]. Normally a liquid meniscus sandwiched between the two parallel surfaces will apply an attractive force on the two surfaces, thereby bringing free resting surfaces closer and hence decreasing the gap between the parallel chips. The evaporation modes of the liquid meniscus in a transient regime are key towards effectively tuning the parameters to achieve a good quality bonding between the surfaces. Ban and Son did a numerical study for a water droplet between the two circular plates for different gaps and temperatures [20]. In all the previous cases, the behavior of the droplet volume during the evaporation phase in a transient regime at room temperature is not well explained in the literature. In various real-world scenarios, the bottom surface is fixed, and the top surface is free-standing with a droplet sandwiched between them. With this paper, we have developed an evaporation model which will address the above-mentioned



Original content from this work may be used under the terms of the [Creative Commons Attribution 4.0 licence](#). Any further distribution of this work must maintain attribution to the author(s) and the title of the work, journal citation and DOI.

research problem. An evaporation model of a droplet sandwiched between the two parallel chips where the bottom chip is fixed, and the top chip is free-standing on the droplet. The top chip will move in the  $z$ -axis with decreasing gap size in the transient regime, as the volume of the droplet decreases due to evaporation at room temperature. The understanding from this study can be used to further develop a theory for, the bonding of silicon chips after water evaporation [21, 22] or gap closure after drying of the water droplet in a capillary gripper [16].

This paper is structured as follows. The motivation and background of this work are first summarized (section 1). Then an evaporation analytical model is developed in section 2, which is used to derive the flux variation along with the air–water interface for decreasing contact angle. Transient decrease in gap and area in the CWA regime and the VWA regime are calculated in section 3. The developed model is then validated with the help of experiments in section 4. Lastly, conclusions and recommendations are made for future work in sections 5 and 6.

## 2. Theory

For a droplet that is confined between two hydrophilic surfaces with negative curvature of the air–water interface, the evaporation involves two main regimes. In the first regime, the wetted area remains constant (that is the droplet is pinned at the edges) [23] and the gap decreases with the evaporation. We call this regime, the constant wetted area (CWA). In the second regime, the wetted area (the overlapping area wetting the top surface of the bottom substrate and the bottom surface of the top chip) between the chips decreases, that is, the contact line recedes. As the wetted area is changing, therefore this regime is referred to as the varying wetted area (VWA). The VWA regime can be influenced by the gap between the chips which may remain constant (due to particle or non-uniform surface morphology) or may decrease further leading to a mixed regime (closing the gap completely and leading to bonding). The time in the VWA regime is highly dependent on the gap and may remain constant for a given gap size and the wetted area. The below-mentioned evaporation model can be adapted for the evaporation of a droplet in a capillary gripper [24].

A fluid sandwiched between two parallel plates with a negative circular curvature is considered for this study. The schematics of the evaporation model is shown in figure 1. A de-ionized water (DIW) layer creates a gap of height  $h$ , sandwiched between chips of size  $2a$ . The ambient temperature of the air is,  $T_{\text{air}}$ , while  $H$  is the relative humidity of the ambient air which is 41% and  $C_v$  is the vapor concentration of the ambient atmosphere and has a value of  $0.0232 \text{ kg m}^{-3}$ .

In this model, the following assumptions are made for the theoretical understanding,

- The top surface of the bottom substrate and the bottom surface of the top chip are completely wetted by DIW and have the same surface energy.

- The chips are completely parallel during evaporation of the DIW.

A simple equation that governs the rate of evaporation per unit area  $F$ , can be derived using Fick's law and is written as,

$$F = -D(T) \cdot \frac{\partial C}{\partial x} \quad (1)$$

where,  $C$  is the concentration of diffusing material,  $x$  is the space coordinate normal to the surface area and  $D(T)$  is the diffusion coefficient as a function of temperature  $T$ . Diffusion coefficient of water is  $24.58 \text{ mm}^2 \text{ s}^{-1}$  at  $22^\circ\text{C}$ . Since the concentration gradient is negative, the minus sign is inserted to get a positive value for the rate of evaporation in the direction of decreasing concentration. The concentration gradient can be given as,

$$\frac{\partial C}{\partial x} = \int_0^h \frac{C_v(1-H)}{r} dS \quad (2)$$

$$r = \frac{h}{2 \cdot \cos \theta}. \quad (3)$$

$C_v$  is the saturated vapor concentration at the air–water interface as a function of temperature  $T$ ,  $r$  is the radius of curvature at the droplet surface (given by equation (3)) and depends on the droplet shape at the liquid–air interface and  $dS$  is the change in surface area (at the liquid–air interface) due to evaporation. With increasing time, the surface area of the water–air interface will decrease as the gap between them will decrease because of the volumetric evaporation of DIW. Therefore, the surface area is related to the gap  $h$  by equation (6).

The rate of evaporation will lead to change in mass of the droplet with time which can be written as below,

$$\dot{m}(t) = \frac{dm}{dt} = \rho(T) \frac{dV}{dt} \quad (4)$$

where  $m$  is the mass of the liquid,  $V$  is the volume of the liquid,  $\rho(T)$  is the density of the liquid as a function of temperature  $T$ . Using equations (1) and (2) in equation (4) we get,

$$\dot{m}(t) = \rho(T) \frac{dV}{dt} = -D(T) \int_0^h \frac{C_v(1-H)}{r} dS. \quad (5)$$

The surface area  $S(h)$  of DIW sandwiched between two parallel plates [26] is given as,

$$S(h) = 8ah - 2 \cdot \frac{h^2}{\cos \theta} \cdot f_1(\theta) \quad (6)$$

where,

$$f_1(\theta) = 2 - \sin \theta - \frac{1}{\cos \theta} \cdot \left( \frac{\pi}{2} - \theta \right) \quad (7)$$

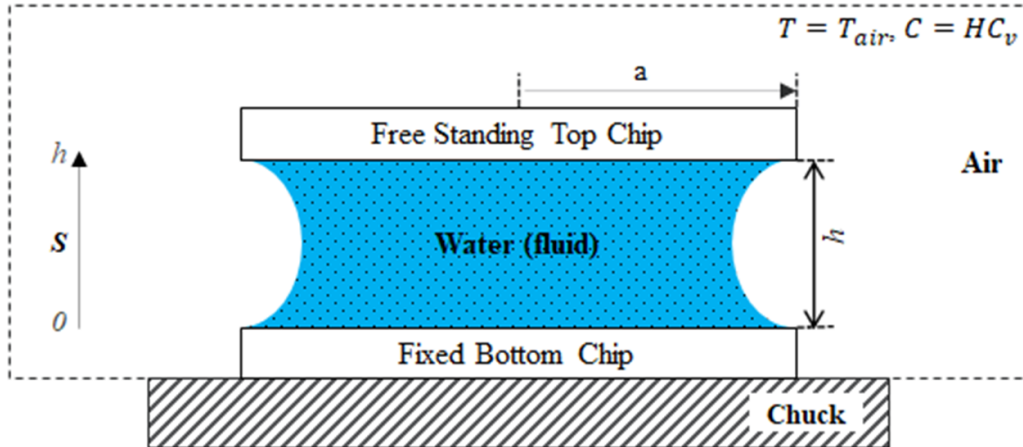


**Figure 1.** Schematic of an evaporation model of a fluid confined between two parallel chips. The bottom chip is fixed on the chuck and the top chip rests on the liquid meniscus and is free to move with decreasing volume of the fluid.

where,  $a$  ( $=5\text{ mm}$ ) is the half of the length of the chip and  $\theta$  is the contact angle of the droplet on the top and bottom chip. In our case, the bottom surface of the top chip and top surface of the bottom substrate have the same surface energy and hence the same contact angle.

Using equations (3) and (6) in equation (5) and integrating, the decreasing mass due to evaporation is given as,

$$m(t) = -8.D(T).C_v(1-H).[2.a.\cos\theta.\ln(h) - h.f_1(\theta)].t. \quad (8)$$

The above equation is the main equation for further investigation of various parameters influencing the evaporation of the droplet. The top chip weighs  $0.175\text{ gm}$  which does not have any significant impact on the meniscus of the droplet DIW.

### 3. Analytical simulation

#### 3.1. Evaporation flux in steady state

The local evaporation flux at the liquid-air interface is expressed as,

$$\vec{J}(h,\theta) = D(T).\vec{\nabla}c. \quad (9)$$

The flux rate of the droplet is heavily dependent on the gap and the contact angle of the droplet at the solid surfaces and can be written as,

$$\vec{J}(h,\theta) = \frac{2.D(T).C_v(1-H).\cos\theta}{h}. \quad (10)$$

For a steady state condition, the flux decreases linearly with every  $5^\circ$  increase in contact angle and increases near the solid–liquid triple contact point as shown in figure 2. Even with increasing contact angle the change in gap ( $\sim$  in  $\mu\text{m}$  range) will be negligible for large ( $\sim$  in  $\text{mm}$  range) die size. The major change in the gap size will come from the increased evaporation flux.

#### 3.2. Influence of the contact angle on the evaporation rate

As indicated in the previous section, the flux decreases with increasing contact angle and this will also influence the evaporation rate  $\dot{m}$  of the meniscus, which is described using equation (8) as,

$$\dot{m} = \frac{dm}{dt} = -8.D(T).C_v(1-H) . [2.a.\cos\theta.\ln(h) - h.f_1(\theta)]. \quad (11)$$

As shown in figure 3, the evaporation rate decreases as  $\theta$  varies from  $0 \rightarrow 90^\circ$ . This is due to the increase in flux at a smaller contact angle when compared to larger contact angle.

#### 3.3. Decrease in gap in CWA regime

Using equations (3), (5), (8) and (9) the change in height  $h(t)$  can be calculated in a CWA regime and is expressed as,

$$h(t) = -4.\frac{D(T).C_v(1-H)}{\rho(T)} . \left[ 2.\cos\theta.\ln(h) - \frac{h}{a}.f_1(\theta) \right].t. \quad (12)$$

Figure 4, plots the decrease in gap between the chips with time. The decreasing gap is linearly dependent on time. It is important to note, that with passing time the contact angle will change, this will lead to deviations from the simulations. Also, a free-standing chip may remain tilted after placement which may lead to deviations from this line. These observations are further discussed in the experimental section. The CWA regime is next followed by VWA regime and this will influence the total time of evaporation which will depend on the fact that the evaporation will lead to bonding between the chips or not.

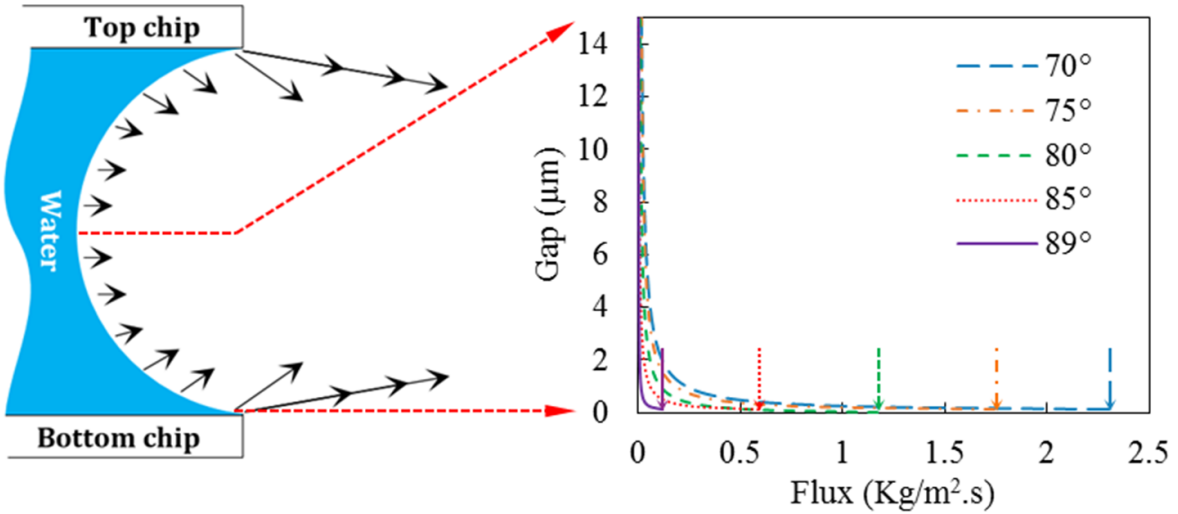


**Figure 2.** The figure on the left is a representation of the flux along with the liquid–air interface for a gap size of  $30 \mu\text{m}$  between the top and bottom chip. The inset shows the magnitude of the evaporation flux along the droplet surface. The y axis shows half of the total gap between the chip as depicted by dotted red arrows. The evaporation flux rate increases at the edge near the meniscus pinning. For a decreasing contact angle, the flux increases and is more significant at the pinning point on the solid surface.

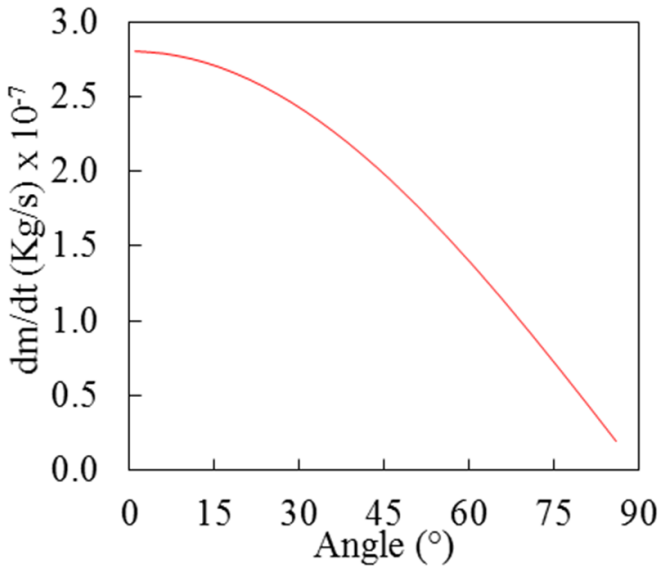


**Figure 3.** Influence of contact angle on the evaporation rate.

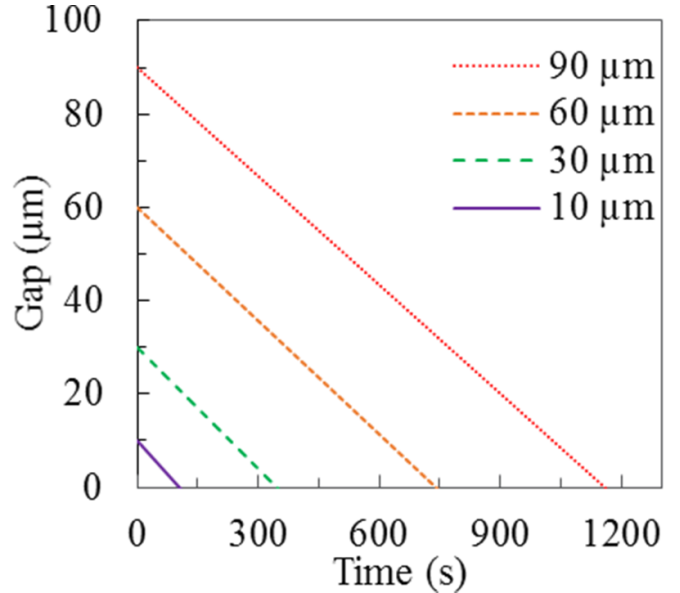


**Figure 4.** The decrease in the gap with time for  $10 \mu\text{m}$ ,  $30 \mu\text{m}$ ,  $60 \mu\text{m}$ , and  $90 \mu\text{m}$  gap.

### 3.4. Decrease in the wetted area in VWA regime

The evaporation rate is highest near the meniscus triple line as already shown in figure 2 and section 3.1. With a decreasing gap, the volume of the fluid to be evaporated is less. Due to the large flux value, evaporation will be faster [28].

Using equations (3), (5)–(7), the change in area at a constant gap is given as,

$$A(t) = 8 \cdot \frac{D(T) \cdot C_V (1 - H)}{\rho(T)} \cdot \left[ 2 \cdot \frac{a_w}{h_c} \cdot \cos \theta + \ln(h_c) \cdot f_1(\theta) \right] \cdot t \quad (13)$$

where,  $h_c$  is the constant gap during evaporation and  $a_w$  is the radius of the water droplet over the surface of chip.

The wetted area for  $10 \text{ mm}$  chip size is  $100 \text{ mm}^2$ . Figure 5(a) plots the decreasing area with increasing time. For a small gap size, it takes less time for the DIW to evaporate completely. A small gap size of the order of one-tenth of a micrometer is considered for any small particle or surface imperfections that may lead to this gap. Figure 5(b) shows that the total evaporation time in the VWA regime is directly dependent on the gap size and increases linearly with an increase in the gap between the chips.

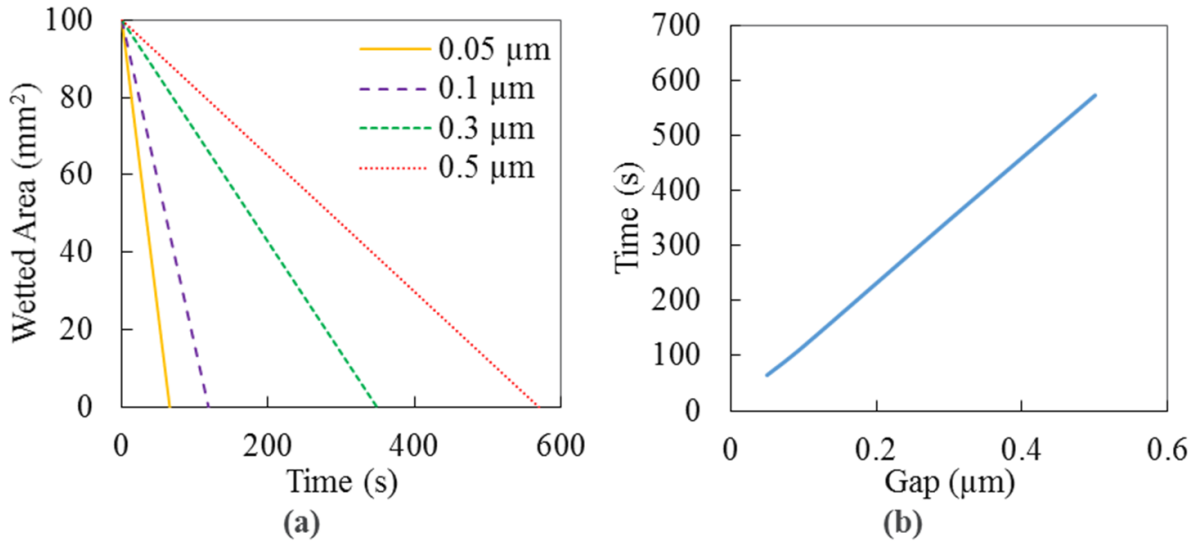


**Figure 5.** (a) Wetted area vs time for varying gaps (50 nm, 100 nm, 300 nm, and 500 nm) between the chips. (b) Time taken for the evaporation of the droplet for varying gap sizes.

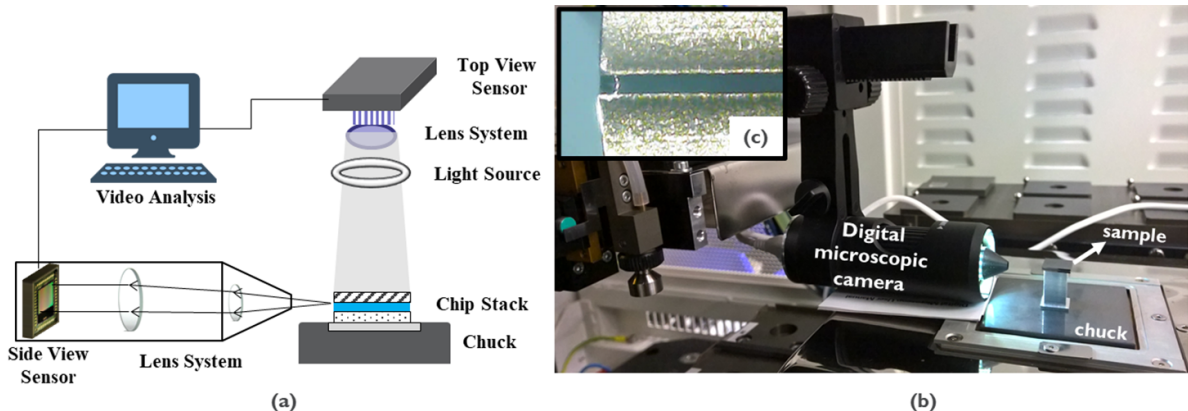


**Figure 6.** (a) Schematic of the measurement setup to inspect the displacement of the top chip during the CWA regime (via side view sensor) and the motion of the meniscus during the VWA regime (via top view sensor). (b) experimental setup showing the measurement in the side view sensor and the inset image (c) showing the liquid between two silicon chips. The liquid meniscus has the curvature towards the bulk of the liquid.

## 4. Experimental validation

### 4.1. Measurement method

To understand the evaporation of water sandwiched between two surfaces, the bottom silicon chip and top glass chip of 10 mm × 10 mm size are used. The fabrication and surface treatment of silicon chip and glass chip is discussed in appendix A (see supplementary (available online at [stacks.iop.org/JMM/32/075001/mmedia](https://stacks.iop.org/JMM/32/075001/mmedia))). The contact angle on the silicon surface and the glass surface (used for observing the VWA regime) is measured to be less than 5° using the Dataphysics OCA-25 goniometer. To study the dynamics of water evaporation between two chips at room temperature, a camera-lens system is used as shown in figure 6. The change in the gap during water evaporation against time in the CWA regime is inspected from the side view sensor (shown in the figures 6(a) and (b)). The area change in the VWA regime is observed from

the top view sensor (shown as schematics in figure 6(a) only). The transparent glass is used to observe the meniscus motion in the VWA regime. The top glass chip has the same size, the bottom surface of which has the same surface treatment leading to the same surface energy as the top surface of the bottom silicon chip. The contact angle on both the surfaces are measured using a goniometer and it was <5°.

### 4.2. Results and comparison

Figure 7 shows the decrease of the gap between the chips for a gap size of 30 μm, 60 μm and 90 μm created by using 3 μl, 6 μl, and 9 μl volume of DIW respectively. The curves obtained from the experiment do not follow a linear path as shown by simulations. The deviation in the curves is due to the tilt of the top chip [29] which is commonly observed for a free-standing top chip. The curve for 9 μl DIW volume

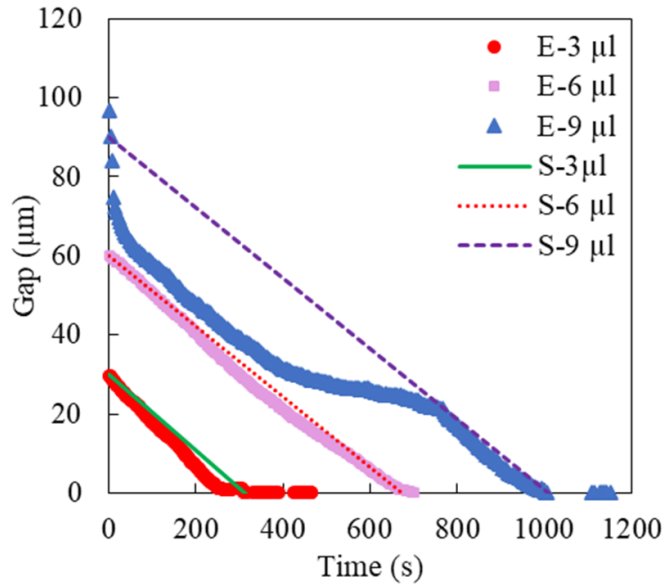


**Figure 7.** Shows the experimental ‘E’ (from the side view sensor) and simulated ‘S’ values in the CWA regime of the decreasing gap between the chips for gap sizes of  $30\ \mu\text{m}$ ,  $60\ \mu\text{m}$ , and  $90\ \mu\text{m}$  corresponding to  $3\ \mu\text{l}$ ,  $6\ \mu\text{l}$  and  $9\ \mu\text{l}$  of water respectively.

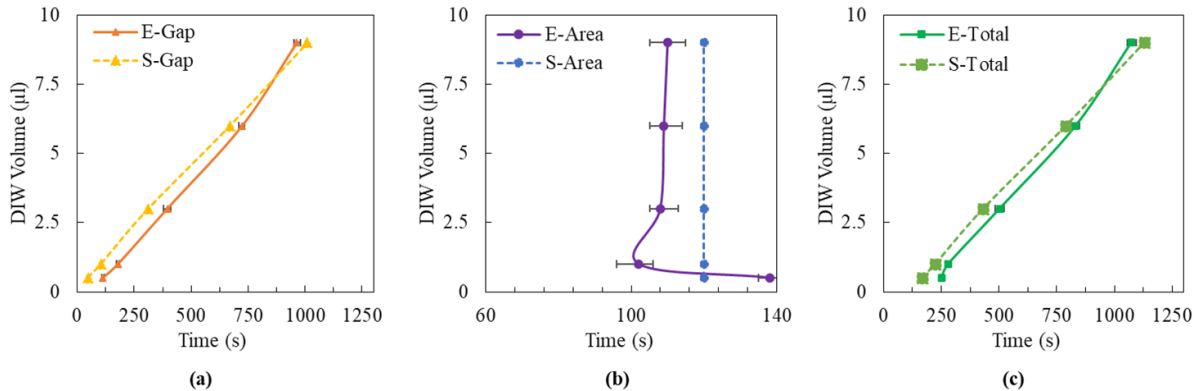


**Figure 8.** Shows the experimental ‘E’ (from the top view camera) and simulated ‘S’ values for total time it takes for various DIW volume. (a) E-Gap refers to the time it takes for the evaporation in the CWA regime, (b) E-Area refers to the time it takes from the onset of the VWA regime to the end of the VWA regime. (c) E-total refers to the total time it takes for the given volume of water to evaporate after the placement of the chip including the time in CWA and VWA.

follows a straight line after it reaches a gap of  $20\ \mu\text{m}$ . Also, in separate experiments, it was observed that the top chip remains parallel to the bottom chip for a small volume ( $<2\ \mu\text{l}$ ) of DIW.

To understand the VWA regime, total evaporation of DIW is observed using a ‘top view sensor’ through the transparent top glass chip. The evaporation time is measured after the placement of the top glass chip for  $0.5\ \mu\text{l}$ ,  $1\ \mu\text{l}$ ,  $3\ \mu\text{l}$ ,  $6\ \mu\text{l}$  and  $9\ \mu\text{l}$  volume of DIW (see figure 8). With increasing volume of DIW the time in the CWA regime increases and evaporation takes more time to reach VWA regime. It takes  $113\text{ s}$ ,  $179\text{ s}$ ,  $395\text{ s}$ ,  $723\text{ s}$  and  $962\text{ s}$  for  $0.5\ \mu\text{l}$ ,  $1\ \mu\text{l}$ ,  $3\ \mu\text{l}$ ,  $6\ \mu\text{l}$  and  $9\ \mu\text{l}$  volume of DIW respectively to transition from CWA regime to VWA regime. The time in VWA regime remains same and varies around  $120\text{ s}$  which means that the DIW lotions inside at a constant gap. The small gap (less than  $1\ \mu\text{m}$ ) during VWA regime is difficult to resolve from the ‘side view image sensor’. The

total time for the complete evaporation of the DIW increases linearly with increasing volume as shown in figure 8(c). The error bar for experiments are shown in each figure but may not be visible due to large time scale.

## 5. Conclusion

In this paper, we developed a transient model for the evaporation of DIW sandwiched between a fixed bottom silicon chip and free-standing top chip. The evaporation is highly dependent on the contact angle at the triple line, the gap between the chips and the size of chip. With decreasing contact angle, the flux increases and hence the evaporation rate. The rate of decrease of gap between the chips in CWA regime and wetted area in VWA regime are linear. This is further validated with the help of experiments.

## 6. Future work

With a decreasing gap, the cooling effect at the air–water interface should trigger the thermo-capillary effect. Which in VWA regime due to small gap and high evaporation flux should increase. The observation of the thermo-capillary effect was not possible in our experimental setup. Also, we suspect an investigation of DIW evaporation in a mixed regime should be of high interest as it may lead to an exciting new understanding of the impact of DIW evaporation on the bonding between the chips.

## Data availability statement

All data that support the findings of this study are included within the article (and any supplementary files).

## ORCID iD

Vikas Dubey  <https://orcid.org/0000-0002-0830-2279>

## References

- [1] Deegan R D, Bakajin O, Dupont T F, Huber G, Nagel S R and Witten T A 1997 Capillary flow as the cause of ring stains dried liquid drops *Nature* **389** 827–9
- [2] Popov Y O 2005 Evaporative deposition patterns: spatial dimensions of the deposit *Phys. Rev. E* **71** 036313
- [3] Bohren C F 1987 *Clouds in a Glass of Beer* (New York: Wiley)
- [4] Houghton H G 1933 A study of the evaporation of small water drops *J. Phys. D: Appl. Phys.* **4** 419
- [5] Sherehovsky J L and Steckler S 1936 A study of the evaporation of small drops and of the relationship between surface tension and curvature *J. Chem. Phys.* **74** 108
- [6] Monchick L and Reiss H 1954 Studies of evaporation of small drops *J. Chem. Phys.* **22** 831
- [7] Peiss C N 1989 Evaporation of small water drops maintained at constant volume *J. Appl. Phys.* **65** 5235
- [8] Kuz V A 1991 Evaporation of small drops *J. Appl. Phys.* **69** 7034
- [9] Birdi K S, Vu D T and Winter A 1989 A study of the evaporation rates of small water drops placed on a solid surface *J. Phys. Chem.* **93** 3702–3
- [10] Dhavalswarupu H K, Migliaccio C P, Garimella G V and Murthy J Y 2010 Experimental investigation of evaporation from low-contact-angle sessile droplets *Langmuir* **26** 880–8
- [11] Dunn G J, Wilson S K, Duffy B R, David S and Sefiane K 2008 A mathematical model for the evaporation of a thin sessile droplet: comparison between experiment and theory *Colloids Surf. A* **323** 50–55
- [12] McHale G, Aqil S, Shirtcliffe N J, Newton M I and Erbil H Y 2005 Analysis of droplet evaporation on a super-hydrophobic surface *Langmuir* **21** 1053–11060
- [13] McHale G, Rowan S M, Newton M I and Banerjee M K 1997 Evaporation and the wetting of a low-energy solid surface *J. Phys. Chem. B* **102** 1964–7
- [14] Pittoni P G, Chang -C-C, Yu T-S and Lin S-Y 2013 Evaporation of water drops on polymer surfaces: pinning, depinning and dynamics of the triple line *Colloids Surf. A* **432** 89–98
- [15] Moriceau H, Rieutord F, Fournel F, Le Tiec Y, Di Cioccio L, Morales C, Charvet A M and Deguet C 2011 Overview of recent direct wafer bonding advances and applications *Adv. Nat. Sci.: Nanosci. Nanotechnol.* **1** 043004
- [16] Lambert P and Delchambre A 2005 Design rules for a capillary gripper in microassembly (*ISATP 2005*). *The 6th IEEE Int. Symp. on Assembly and Task Planning: From Nano to Macro Assembly and Manufacturing, 2005* pp 67–73
- [17] Chafaï A, Vitry Y, Dehaeck S, Gallaire F, Scheid B, Colinet P and Lambert P 2021 Two-dimensional modelling of transient capillary driven damped micro-oscillations and self-alignment of objects in microassembly *J. Fluid Mech.* **910** A6
- [18] Leng J 2010 Drying of a colloidal suspension in confined geometry *Phys. Rev. E* **82** 021405
- [19] Clement F and Leng J 2004 Evaporation of liquids and solution in confined geometry *Langmuir* **20** 6538–41
- [20] Ban H and Son G 2015 Numerical simulation of droplet evaporation between two circular plates *J. Mech. Sci. Technol.* **29** 2401–7
- [21] Dubey V, Derakhshandeh J, Beyne E, Celis J P and De Wolf I 2016 Fine pitch rapid heat self-aligned assembly and liquid-mediated direct bonding of Si chips *IEEE Trans. Compon. Packag. Manuf. Technol.* **6** 946–53
- [22] Dubey V *et al* 2016 Liquid mediated direct bonding and bond propagation *2016 6th Electronic System-Integration Technology Conf. (ESTC) (Grenoble)* pp 1–4
- [23] Oliver J F, Huh C and Mason S G 1977 Resistance to spreading of liquids by sharp edges *Journal of Colloid and Interface Science* **59** 568–81
- [24] Arutinov G, Smits E C P, Albert P, Lambert P and Mastrangeli M 2014 In-plane mode dynamics of capillary self-alignment *Langmuir* **30** 13092–102
- [25] Jones F E and Harris G L 1992 ITS-90 density of water formulation for volumetric standards calibration *J. Res. Natl Inst. Stand. Technol.* **97** 335–40
- [26] Dubey V, Beyne E, Derakhshandeh J and De Wolf I 2017 Physics of self-aligned assembly at room temperature *Physics of Fluids* **30** 01200
- [27] Gatapova E Y, Semenov A A, Zaitsev D V and Kabov O A 2014 Evaporation of a sessile water drop on a heated surface with controlled wettability *Colloids Surf. A* **441** 776–85
- [28] Buffione C and Sefiane K 2004 IR measurements of interfacial temperature during phase change in a confined environment *Exp. Therm Fluid Sci.* **29** 65–74
- [29] Abbasi S, Zhou A X, Baskaran R and Bohringer K F 2008 Part tilting in capillary-based self-assembly: Modeling and correction methods *International Conference on Micro Electro Mechanical Systems 21st Conf. on MEMS 2008 (Tucson, AZ, 13–17 January 2008)* pp 1060–3